Spin-1/2 Ising ladder with randomly coupled rung interaction and transverse magnetic field

Maria Eugênia Silva Nunes[1,2,*] and J. A. Plascak[3,4,5,†]

[1]*Departamento de Física, ICEB, Universidade Federal de Ouro Preto, Campus Universitário Morro do Cruzeiro, 35400-000 Ouro Preto, MG, Brazil*

[2]*Centro de Desnvolvimento da Tecnologia Nuclear, C.P. 941, 30161-970 Belo Horizonte, MG, Brazil*

[3]*Departamento de Física, Instituto de Ciências Exatas, Universidade Federal de Minas Gerais, C.P. 702, 30123-970 Belo Horizonte, MG, Brazil*

[4]*Universidade Federal da Paraíba, Centro de Ciências Exatas e da Natureza, Campus I, Departamento de Física, CCEN Cidade Universitária, 58051-970 João Pessoa, PB, Brazil*

[5]*Center for Simulational Physics, University of Georgia, Athens, Georgia 30602, USA*

(Received 22 September 2023; revised 22 December 2023; accepted 2 January 2024; published 23 January 2024)

The quantum spin-1/2 Ising ladder with homogeneous side rail interaction and disordered rung interaction in the presence of a random site transverse magnetic field has been studied using the method of recurrence relations in the high-temperature limit. The first six recurrants have been exactly calculated, and a linear extrapolation process has been used to obtain a total of 100 recurrants. This extrapolation allows us to extend the analysis to longer times. Both the rung coupling and the transverse field obey a bimodal distribution. The time autocorrelation functions of the z-component dynamic spin variable have been obtained. We have considered several cases of rung and transverse field distributions, as well as several values of the Hamiltonian parameters. The results show that the disorder present in the rung interaction and external transverse field affects the behavior of the temporal autocorrelation and the spectral functions in all studied cases. In addition, the interesting case where the rung interactions and the transverse magnetic field are correlated has also been studied. In general, transition in the dynamics of the system from individual to collective mode was observed depending on the dominant kind of interaction in the sites, that is, whether most of the sites were subject to a strong external field or strong interchain local interactions.

DOI: 10.1103/PhysRevE.109.014134

I. INTRODUCTION

Since the ancient use of natural magnets as compass for orientation, magnetic materials have been widely used in several important technological applications. Nowadays, there has been a great interest in integrated microscopic devices [1]. However, for such devices to be viable, it is necessary to search for materials that can further carry electron spin current. In order to achieve this viability, it has been noticed that a strong correlation between spins is required to obtain spin current transport in microscopic devices [1].

Besides the spintronic properties there is also technological interest in high-temperature superconductors. A significant number of works in the literature concern not only the synthesis of these compounds but also the study of their thermodynamic properties. For example, Johnston *et al.* [2] synthesized the polycrystal $(VO)_2P_2O_7$, which behaves like a Heisenberg quantum ladder. They also measured its magnetic susceptibility at temperatures between 4 and 350 K. Hagiwara *et al.* [3] measured the magnetic behavior of the $Cu(C_5H_{12}N_2)_2Cl_4$ crystal, which could be well described by a spin-1/2 Heisenberg ladder type for temperatures below 0.5 K and magnetic fields about 12 T.

It has been recently discovered that the spin-lattice interaction plays also an important role in spintronic compounds. Arisawa *et al.* [4] showed that the $Tb_{0.3}$ $Dy_{0.7}Fe_2$ magnet exhibits strong spin-lattice coupling, implying a magnetostriction-like effect, where in this case the volume changes when a spin current is injected by spin Hall effects. The above aspects clearly show how important it is to have a better understanding of the interactions between spins and their neighborhood in such materials. Moreover, a better understanding of ladder-type structured systems can surely lead to a better understanding of superconductors and, hopefully, spintronic effects as well.

It is well known that previous theoretical studies of low-dimensional systems have opened up novel interesting paths of investigation in quantum spin models. For instance, in recent decades, several quasi-one-dimensional composites have been synthesized in laboratory, and their properties could be well described by one-dimensional Heisenberg, *XXZ*, *XY*, or Ising-type magnetic models. In this direction, we can cite $BaCo_2V_2O_8$ [5,6], Cs_2CoCl_4 [7], and $SrCo_2V_2O_8$ [8] compounds, among so many others. There are some experimental works in the literature regarding the interactions that can arise between the couplings and the external magnetic field in low-dimension systems. For example, in the work of

*mariaeugenia@ufop.edu.br
†pla@uga.edu, pla@fisica.ufmg.br

Pogoryelov [9] and Gomonay [10], it has been discussed how the external magnetic field can affect the strength of the couplings.

It is also worthwhile to mention the versatility of such quantum models that can also be applied in the description of the dynamics of ferroelectric hydrogen bonded crystals such as CsH_2PO_4 and its deuterated CsD_2PO_4 form [11–16]. The transverse Ising-like models, suitable for these systems, has indeed been originally proposed to describe the tunneling effects present in KH_2PO_4 and KD_2PO_4 ferroelectric compounds [17].

From the above discussion, it is not surprising that there are, from a theoretical point of view, many works in the literature addressing the magnetism of low-dimensional quantum systems, in their static and dynamical nature, using different approximative analytical and computational tools. However, due to the complex nature of the quantum interactions, one has exact results for only a few models. For instance, the time-dependent pair correlation functions have been rigorously obtained for the transverse Ising [18] and *XY* [19–21] chains, while the dynamic structure factor has been studied for the *XXZ* Heisenberg chain [22–25]. Exact results have also been obtained in the study of various interesting Ising-Heisenberg spin models on a ladder structure [26–32].

Numerical approaches to examine the dynamics of quantum chain models based on the Jordan-Wigner fermionization have been proposed [33–35] and applied to the transverse Ising and *XY* models, including random situations [15,36,37], and also a comparison to rigorous predictions [16,38].

It has also been noticed that several of the theoretical works concern the application of the recurrence relations method (RRM) to the study of the dynamics of the spin autocorrelation function [39–44]. Specifically regarding the ladder structure, Krimphoff *et al.* [45] investigated the propagation dynamics in the spin-1/2 isotropic Heisenberg ladder. The system starts from an initial state with two localized overturned neighboring spins, either in one of the chains or in a rung in a ferromagnetic background. They have found that, compared to the corresponding dynamics in a single chain, there are several additional modes of propagation of the perturbance in the whole ladder. Recently Yuan *et al.* [46] studied the influence of correlated transverse and longitudinal magnetic fields on the dynamical behavior of the Ising chain. They observed that such fields have enormous influence on the correlation and spectral functions of the system.

Due to the importance of the spin interactions in so many magnetic systems and devices, we have studied in this work a ladder consisting of two spin-1/2 Ising chains that interact with each other via a random site-dependent rung coupling. The ladder is in the presence of an external transverse magnetic field, which is also randomly site dependent. The goal is to investigate the time-dependent z-component autocorrelation function and its spectral function through the use of the recurrence relations method. The rung coupling and the transverse field obey a bimodal distribution. Although independent distributions can, in general, be treated, one interesting case turns out to be when both rung coupling and transverse field are correlated to each other.

In order to obtain the z-component autocorrelation function and its spectral function, we have exactly computed the first six recurrants. To extend the time interval, an extrapolation process has been used, where a total 100 recurrants could be used.

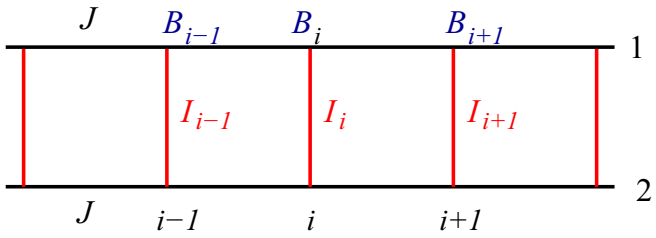

FIG. 1. Part of the infinite ladder structure. J is the interaction along the side rails 1 and 2, I_i is the random interaction of the rung i, and B_i is the corresponding random transverse field acting in both spins of the rung i.

The plan of the paper is the following. In the next section we define the general model on a ladder structure as well as the bimodal probability distributions. In Sec. III we briefly present the recurrence relations method for obtaining the autocorrelation and spectral functions. The extrapolation process is presented in Sec. IV, where a comparison to the one-dimensional transverse Ising model and the transverse Ising ladder with different rung interactions are presented. Secs. V, VI, and VII are devoted to the results for other different types of the Hamiltonian parameters and probability distributions. In Sec. VIII dilution in both the transverse field and rung interaction is analyzed. Some final comments are addressed in the last section.

II. HAMILTONIAN OF THE ISING LADDER IN A TRANSVERSE FIELD

The quantum Ising model defined on a ladder structure and in the presence of a transverse magnetic field can be described by the following Hamiltonian:

$$H = -\frac{1}{2}\sum_{i=1}^{N} J\left[\sigma_{i,1}^{z}\sigma_{i+1,1}^{z} + \sigma_{i,2}^{z}\sigma_{i+1,2}^{z}\right] + \frac{1}{2}\sum_{i=1}^{N} I_i\sigma_{i,1}^{z}\sigma_{i,2}^{z} - \frac{1}{2}\sum_{i=1}^{N} B_i\left[\sigma_{i,1}^{x} + \sigma_{i,2}^{x}\right], \quad (1)$$

where the index i labels the rung connecting the side rails 1 and 2, as in Fig. 1, and we are in the thermodynamic limit, $N \to \infty$. In the above expression, J is the exchange coupling along the two side rails, I_i is a random bond-dependent rung interaction, B_i is a random site-dependent transverse magnetic field acting on the pair of sites belonging to the rung i, and $\sigma_{i,a}^{\alpha}$, with the components $\alpha = x, y, z$ and side rails $a = 1, 2$, are Pauli spin matrices.

The random bond and the random site transverse field are given, respectively, by the following bimodal distribution functions:

$$P_b(I_i) = p_b\delta(I_i - I_A) + (1 - p_b)\delta(I_i - I_B), \quad (2)$$

$$P_t(B_i) = p_t\delta(B_i - B_A) + (1 - p_t)\delta(B_i - B_B), \quad (3)$$

where p_b is the probability of having a rung bond of strength I_A and $1-p_b$ is the probability of having a rung bond of strength I_B. Similarly, p_t is the probability of having a transverse field on both spins of the rung of strength B_A and $1-p_t$ is the probability of having a transverse field on both spins of the rung of strength being B_B.

Several particular cases can be obtained from the above general distributions of the transverse field Ising model in a ladder. Some instances are described by the following:

(i) $I_A = I_B \neq J$ and $B_A = B_B = B$ correspond to a uniform transverse field with rung interactions different from the rail interactions (it is a pure model, because of the independence of the equations upon the probabilities p_b and p_t).

(ii) $I_A \neq I_B$ and $B_A = B_B = B$ correspond to a uniform transverse field with random rung interactions having two different values (in this case, independent on p_t).

(iii) $I_A = I_B = J$ and $B_A \neq B_B$ correspond to an isotropic ladder with random transverse field having two different values (in this case, independent on p_b).

(iv) $I_B = 0$ and $B_A = B_B$ correspond to a uniform transverse field with diluted rung interactions (independent of p_t).

(v) $p_b = p_t = p$ and $I_B = 0$ and $B_A = 0$ correspond to an interesting case of rung bond and transverse field correlated distribution. It means that when $p = 0$ we have two independent Ising chains in a transverse field, and when $p = 1$ we just have the classical Ising model in a ladder.

(vi) $I_A \neq I_B$ and $B_A \neq B_B$ correspond to a ladder with an independent random transverse field and random rung interaction (in this case, simultaneously dependent on both p_b and p_t).

According to the distributions expressed in (2) and (3), any function $f(I_i, B_i)$ that is dependent on the random rung bonds I_i and on the random transverse fields B_i variables has its average value over the disorder obtained by computing

$$\overline{f(I_i, B_i)} = \int P_b(I_i) P_t(B_i) f(I_i, B_i)\, dI_i\, dB_i. \tag{4}$$

Some of the above models will be treated using the recurrence relations method, which will be outlined in the next section. In all of them, the function $f(I_i, B_i)$ will be the temporal autocorrelation function of the z-component spin operator.

III. RECURRENCE RELATIONS METHOD

The dynamics of the present model will be studied by using the recurrence relations method (RRM) formulated by Lee [47,48] in 1982. This method has been shown to be quite useful in obtaining the dynamics of many body systems. The RRM is based on the Gram-Schmidt [49,50] process of orthogonalization, which allows the construction of a complete set of orthogonalized vectors in a Hilbert space. As this method has already been used in diverse systems, we will describe below just the main points to obtain the spin autocorrelation function and its spectral function.

For any operator A corresponding to a given observable, we have in the Heisenberg representation its time dependence given by $A(t) = e^{iHt} A(0) e^{-iHt}$, with $A(0) \equiv A$, and in a unit system where $\hbar = 1$. Thus, the temporal evolution of A is governed by the Liouville equation

$$\frac{dA(t)}{dt} = iLA(t), \tag{5}$$

with the Liouville operator $LA = [H, A] \equiv HA - AH$ and H is the Hamiltonian of the system.

In the RRM, $A(t)$ is viewed as a vector defined in a Hilbert space of dimension d. The size of this space depends on the system under study and on the specific dynamical variable. The metric in this space is defined by the Kubo scalar product [51,52]

$$(X, Y) = \frac{1}{\beta} \int_0^\beta \langle X(\lambda) Y^\dagger \rangle d\lambda - \langle X \rangle \langle Y^\dagger \rangle, \tag{6}$$

where X and Y are vectors defined in this Hilbert space, $\beta \equiv 1/(k_B T)$, with k_B the Boltzmann constant and T the temperature. The λ dependence of the vectors is given by $X(\lambda) = e^{\lambda H} X e^{-\lambda H}$ (and similarly for the adjunct operator $Y^\dagger$) and the brackets $\langle \cdots \rangle$ stand for the canonical ensemble average. For instance, for the vector X we have

$$\langle X \rangle = \frac{\mathrm{Tr} e^{-\beta H} X}{\mathrm{Tr} e^{-\beta H}}. \tag{7}$$

In the high-temperature limit, $T \to \infty$, the scalar product reduces to

$$(X, Y) = \frac{\mathrm{Tr} X Y^\dagger}{\mathrm{Tr} 1} = \frac{\sum_n n X Y^\dagger n}{\sum_n n | n}, \tag{8}$$

where n is a complete set of eigenvectors with Tr1 the number of eigenvectors of the system.

The dynamical operator $A(t)$ can be written in a basis in the Hilbert space as

$$A(t) = \sum_{\nu=0}^{d-1} a_\nu(t) f_\nu. \tag{9}$$

In the above equation, the vectors f_ν constitute a complete and orthogonal set, but non-normalized, satisfying what is called recurrence relation I (RRI), namely,

$$f_{\nu+1} = iLf_\nu + \Delta_\nu f_{\nu-1}, \tag{10}$$

with

$$\Delta_\nu = \frac{(f_\nu, f_\nu)}{(f_{\nu-1}, f_{\nu-1})}. \tag{11}$$

We also have the additional definitions $f_{-1} \equiv 0$ and $\Delta_0 \equiv 1$.

In the above equations, the choice of the first base vector is arbitrary. In general, it is chosen $f_0 = A(0)$. Since the expansion of $A(t)$ in terms of the base vectors f_ν satisfies the Liouville equation, the use of the recurrence relation RRI generates a second recurrence relation RRII given by

$$\Delta_{\nu+1} a_{\nu+1}(t) = -\frac{da_\nu(t)}{dt} + a_{\nu-1}(t), \tag{12}$$

where $0 \leqslant \nu \leqslant d-1$

We can note that the quantities Δ_ν are the only elements that enter into the construction of the terms $a_\nu(t)$, which by their turn completely determine the time evolution of the operator under question.

The term $a_0(t)$ can be, in fact, identified as the time-dependent z-component autocorrelation function $C(t)$:

$$a_0(t) = \left(\sigma_j^z, \sigma_j^z(t)\right) = \frac{1}{Z}\mathrm{Tr}\sigma_j^z\sigma_j^z(t) \equiv C(t). \tag{13}$$

Since we are in the infinite temperature regime, the temporal correlation function for spin operators in different sites of the lattice is zero for any value of time. This implies that the only nonzero quantity of interest is the autocorrelation function. In addition, we can write the time-dependent function $C(t)$ as the inverse Laplace transform of $\alpha_0(z)$,

$$C(t) = \int_0^\infty \alpha_0(z)e^{zt}\,dz, \tag{14}$$

where $\alpha_0(z)$ is written in the continued fraction form

$$\alpha_0(z) = \cfrac{1}{z + \cfrac{\Delta_1}{z + \cfrac{\Delta_2}{z + \cdots}}}. \tag{15}$$

The above continued fraction representation is quite useful in obtaining the desired spectral behavior for the autocorrelation functions.

We can also compute the spectral density $S(\omega)$, defined as the time Fourier transform of the correlation function $C(t)$:

$$S(\omega) = \int_{-\infty}^{+\infty} C(t)e^{-i\omega t}\,dt. \tag{16}$$

However, the spectral density is most directly obtained from the relation [53,54]

$$S(\omega) = \lim_{\epsilon\to 0^+} \mathrm{Re}[2\alpha_0(\epsilon - i\omega)], \tag{17}$$

where Re stands for taking the real part of the complex number.

In order to obtain the correlation and spectral functions we have computed the vectors f_ν up to $\nu = 6$. The first three vectors (for $\nu = 0$ we have just the z-component spin operator), as a function of the rung random interactions and site random transverse field, are given as follows:

$$f_0 = \sigma_{j,1}^z, \tag{18}$$

$$f_1 = -B_j\sigma_{j,1}^y, \tag{19}$$

$$f_2 = B_j\left[J\left(\sigma_{j,1}^x\sigma_{j+1,1}^z + \sigma_{j-1,1}^z\sigma_{j,1}^x\right) - I_j\sigma_{j,1}^x\sigma_{j,2}^z\right], \tag{20}$$

$$\begin{aligned} f_3 = {} & -JB_j\left(B_{j+1}\sigma_{j,1}^x\sigma_{j+1,1}^y + B_{j-1}\sigma_{j-1,1}^y\sigma_{j,1}^x\right) \\ & + B_j\left(B_jI_j\sigma_{j,1}^x\sigma_{j,2}^y + 2J^2\sigma_{j-1,1}^z\sigma_{j,1}^y\sigma_{j+1,1}^z\right) \\ & - 2B_jJI_j\left(\sigma_{j,1}^y\sigma_{j+1,1}^z\sigma_{j,2}^z + \sigma_{j-1,1}^z\sigma_{j,1}^y\sigma_{j,2}^z\right). \end{aligned} \tag{21}$$

For $\nu \geqslant 4$ the expressions are rather lengthy to be reproduced here.

The results obtained from the present procedure will be discussed below. However, before presenting the dynamical behavior for the more general model, it is quite convenient first to see, in the next section, what the present approach furnishes in interesting particular cases, some of them already treated in the literature.

One special case, where exact results can be easily obtained, is the zero field limit, i.e., $B_A = B_B = 0$, which corresponds to the classical Ising model. Therefore, one has $C(t) = 1$ for all times, since in this specific case $f_1 = 0$, $\Delta_1 = 0$, $a_0(z) = 1/z$, and the inverse Laplace transform provides $C(t) = \mathfrak{L}^{-1}a_0(z) = 1$. Thus, there is no dynamics in the classical system for any values of the rung interaction, as expected.

In all Hamiltonian parameter and probability distribution choices below, we will consider $J = 1$. This means, in other words, that we are measuring all interactions and fields in units of the rail interaction J. Accordingly, the time is measured in units of the inverse of the exchange interaction J^{-1}.

IV. UNIFORM TRANSVERSE ISING LADDER WITH DIFFERENT RUNG COUPLINGS: $I_A = I_B = I$ AND $B_A = B_B = B$

For $I_A = I_B = I$ and $B_A = B_B = B$, we have the simple Ising ladder in a homogeneous transverse field with different rung couplings. This is indeed a pure system, because it is independent of the probability distributions (2) and (3). This case has already been recently studied within the RRM by de Souza, de Mello Silva, and Martins [53] (just consider, in this reference, vanishing four-spin interactions).

A. Exact values for Δ_ν with $\nu \leqslant 6$

The first six Δ_ν have been exactly calculated for the system using the RRI and RRII recurrance relations. Just to have an idea of what one gets in this case we have

$$\begin{aligned} \Delta_1 &= \frac{(f_1, f_1)}{(f_0, f_0)} = B^2, \\ \Delta_2 &= \frac{(f_2, f_2)}{(f_1, f_1)} = 2J^2 + I^2, \\ \Delta_3 &= \frac{(f_3, f_3)}{(f_2, f_2)} = \frac{2J^2(B^2 + 2J^2 + 4I^2) + B^2I^2}{2J^2 + I^2}. \end{aligned} \tag{22}$$

In an analogous way, lengthier expressions are obtained for higher values of ν.

Figure 2 shows the first six exact values of Δ_ν for $I_A = I_B = I$ and $B_A = B_B = B$, with $J = 1$ and $B = 1$. For $I = 0$ one has the rails decoupled, leading to the one-dimensional transverse Ising model. As I increases, so does Δ_ν, for all values of ν, and a kind of linear behavior is seen as a function of ν.

The time-dependent spin autocorrelation functions $C(t)$ are then evaluated from these exact six recurrants. The autocorrelation functions, as a function of t, are depicted in Fig. 3 for some values of the rung interaction I. In this case, reliable results could be obtained only up to time $t \sim 0.8$. One can see that as the rung interaction is increased, the decay becomes slower, which is better seen in the inset of Fig. 3.

B. Extrapolation process for $\nu > 6$

In order to extend the autocorrelation function $C(t)$ analysis to a region comprising longer times, a recurrant extrapolation mechanism can be used. It can be seen in Fig. 2 that the growth of the recurrants is approximately linear with

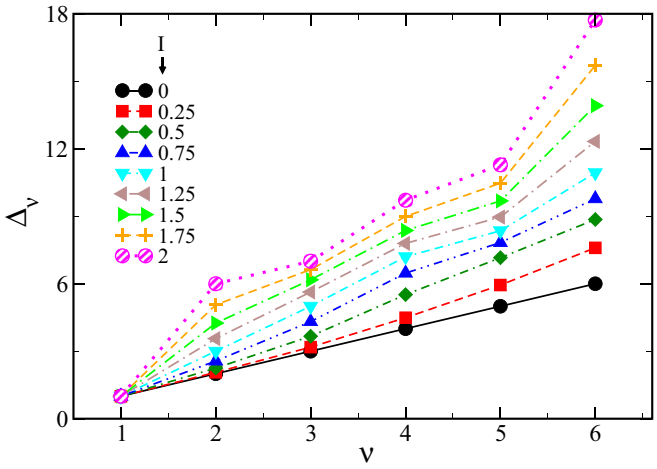

FIG. 2. The first six exact values of Δ_ν for $B = 1$ and different values of I (given, respectively, by the numbers in the legend). In this case we have $I_A = I_B = I$ and $B_A = B_B = B$. The lines are just guides for the eye.

ν. Although as I increases there are noticeable fluctuations of Δ_ν for small values of ν, we expect an alignment for higher order recurrants. In fact, there are several studies in the literature that show this kind of linear growth of the recurrants in Ising-type models [55–59]. Therefore, a linear extrapolation seems to be suitable to obtain more recurrants in each considered case. This extrapolation process can be done by fitting the data to the expression

$$\Delta_\nu = a\nu + b, \tag{23}$$

where $\nu \leqslant 6$ and a and b are fitted constants for each case. In what follows, 100 recurrants have been used by considering the above equation for $7 \leqslant \nu \leqslant 100$. The choice of a maximum of $\nu = 100$ has been based on the fact that the results present no significant changes by taking higher order extrapolated recurrants.

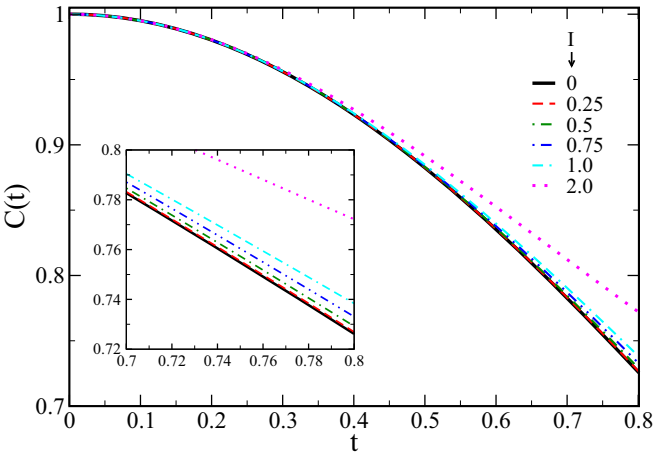

FIG. 3. Time-dependent spin autocorrelation functions $C(t)$ as a function of time t for some values of the rung interaction I shown in Fig. 2. The inset shows a closer view for the longer times that can be reached using only the first six recurrants. The legend and the axes labels of the main graph also applies to the inset.

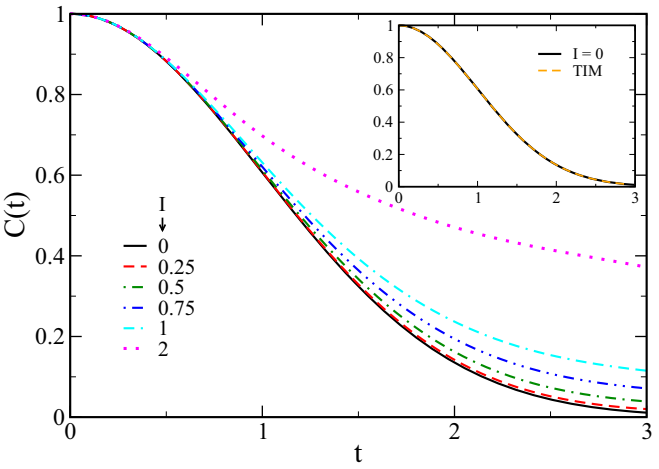

FIG. 4. Time-dependent autocorrelation functions $C(t)$ as a function of time t for the same values of the rung interaction I shown in Fig. 3. In this case we have used 100 recurrants according to the described extrapolation process. The inset shows the autocorrelation function for $I = 0$ compared to the expected value of the one-dimensional transverse Ising model (TIM) from the literature (dashed-line). The axes labels of the main graph also apply to the inset.

Figure 4 shows the autocorrelation functions $C(t)$ so obtained using 100 recurrants and for the same values of the rung interactions as in Fig. 3. It can be seen that the time range has now been extended up to $t \sim 3$. It is also more apparent the slower decay of the autocorrelation function as the rung interaction increases from zero.

The inset in Fig. 4 shows the autocorrelation function for $I = 0$ in comparison to the expected results for the one-dimensional transverse Ising model from the literature, namely, $C(t) \sim e^{-t^2/2}$ for $B = 1$ [19,21]. It is clearly seen that the present results are in excellent agreement in the entire time interval, with the full and dashed lines completely superposed in the scale of the graph. We should then expect a similar behavior for other values of the Hamiltonian parameters and probability distributions up to the time where reliable results could be obtained with $\nu = 100$.

As a matter of further comparison, it should be stressed that the first five recurrants here obtained are exactly the same as those from de Souza, de Mello Silva, and Martins [53] (when the four-spin interaction in Ref. [53] is set to zero and the interactions and transverse field are properly renormalized). The dynamical behavior is also similar. However, in the present case we have one more exact recurrant. Due to the different definition of the Hamiltonian, the timescale here is different from that in Ref. [53].

The observed slower decay in Fig. 4 with the rung interaction is ascribed to the fact that, as I increases, the quantum fluctuations become less dominant and the behavior of the system is in some sense driven to the classical regime. Eventually, in the $I \to \infty$ limit, the autocorrelation function tends to $C(t) \to 1$, for any value of the time t, and the dynamical behavior is completely suppressed.

With a longer time behavior of the autocorrelation function, it is possible to compute the spectral function $S(\omega)$. The

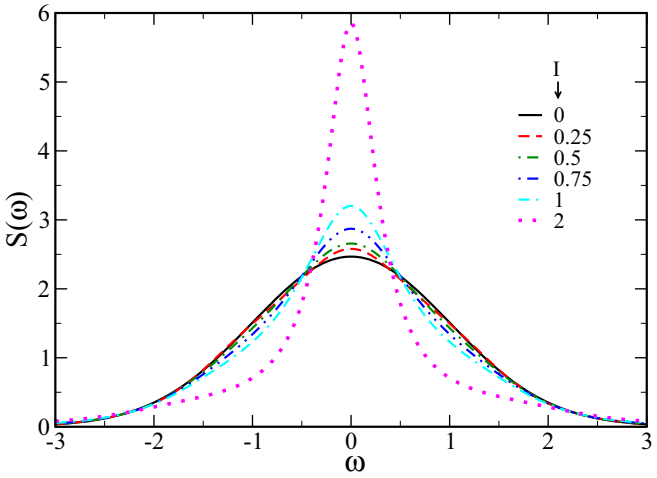

FIG. 5. Spectral functions $S(\omega)$ as a function of ω for $B = 1$ and same values of the rung interaction given in Fig. 4.

corresponding spectral function is shown in Fig. 5 for the same values of the rung interaction used in Fig. 4. One can see that there is a well-pronounced central peak in all cases around the frequency $\omega = 0$. As I increases, the intensity increases with the central peak becoming narrower, emphasizing the dominant central mode behavior. Compatible with the autocorrelation function of Fig. 4, when $I \to \infty$ the spectral function tends to a delta function at $\omega = 0$.

The results for a higher value of the transverse field, $B = 2$, are shown in Fig. 6 for the same values of the rung interaction as before. It is seen that now, even for $I = 2$, the autocorrelation function still decays to negative values. Nevertheless, as expected, as I increases the decay becomes slower and the classical regime will eventually be reached as $I \to \infty$.

The respective spectral functions are depicted in Fig. 7. In this figure it is more clearly seen the tendency of collective modes up to the value $I = 2$. The change to the central peak regime occurs for rung interactions $I > 2$.

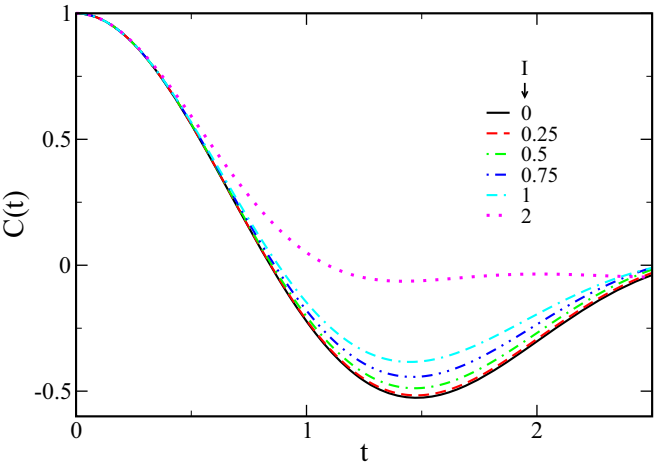

FIG. 6. Time-dependent autocorrelation functions $C(t)$ as a function of time t for the same values of the rung interaction I as before (given by the numbers in the legend). In this case we have $B = 2$.

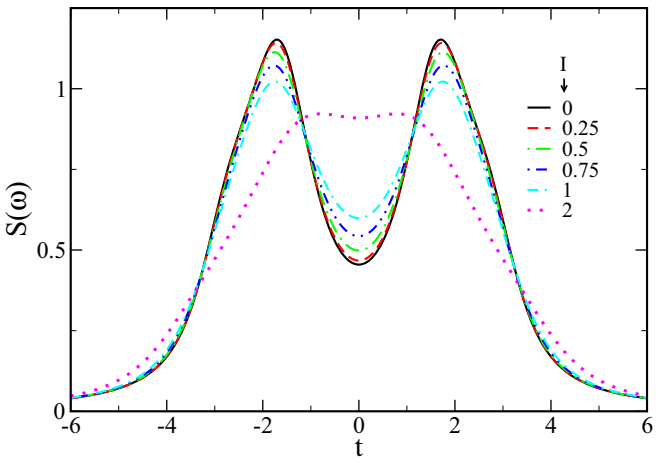

FIG. 7. Spectral functions $S(\omega)$ obtained from the autocorrelation functions shown in Fig. 6 for $B = 2$.

Although the general trend of the dynamical behavior of the uniform transverse Ising ladder seems to be similar to the transverse Ising chain, some basic differences can be noticed regarding the dynamics below and above the ground state critical transverse field. In the transverse Ising chain, it is well known that for $B < B_c^{\text{chain}}$, where $B_c^{\text{chain}} = 1$, one has central-peak-type behavior, while for $B > B_c^{\text{chain}}$ collective-mode types are present (see, for instance, Ref. [58]). In the present case, for $I = 1$, the ground-state critical transverse field is $B_c^{I=1} = 1.8322(2)$ [60,61]. So, for $I = 1$, a central peak is clearly seen in Fig. 5 for $B = 1 (< B_c^{I=1})$, and a collective mode is seen in Fig. 7 for $B = 2 (> B_c^{I=1})$. However, as we shall see in Sec. VI, even for $B = 1.5$, which is still smaller than the critical transverse field, one has a kind of collective-mode behavior (see Fig. 12 and $p_t = 0$).

The entire extrapolation process, that has been done in this subsection, will be followed below in all the other choices for the Hamiltonian parameters and probability distributions.

V. UNIFORM TRANSVERSE ISING LADDER WITH RUNG DILUTION: $I_A = I$, $I_B = 0$ AND $B_A = B_B = B$

With the choice $I_A = I$ and $I_B = 0$ we have rung dilution with probability p_b. We will consider a uniform transverse field $B_A = B_B = B$, implying the dynamics is independent of p_t. In this case the first three recurrants are given by

$$\Delta_1 = B^2,$$
$$\Delta_2 = 2J^2 + p_b I^2,$$
$$\Delta_3 = \frac{2J^2(B^2 + 2J^2 + 4p_b I^2) + B^2 p_b I^2}{2J^2 + p_b I^2}. \tag{24}$$

The next three recurrants Δ_4, Δ_5, and Δ_6 have also been exactly calculated. Notice that now, as the rung couplings are site dependent, the expressions for the recurrants are dependent on the probability p_b. Of course, $p_b = 1$ leads to the previously studied model.

In Fig. 8 it is shown the first six exact recurrants for $B = 1$, $I = 1$, and different values of the rung probability p_b. When $p_b = 0$ we recover the one-dimensional transverse Ising model, the same as $I = 0$ in the previous section. On the other

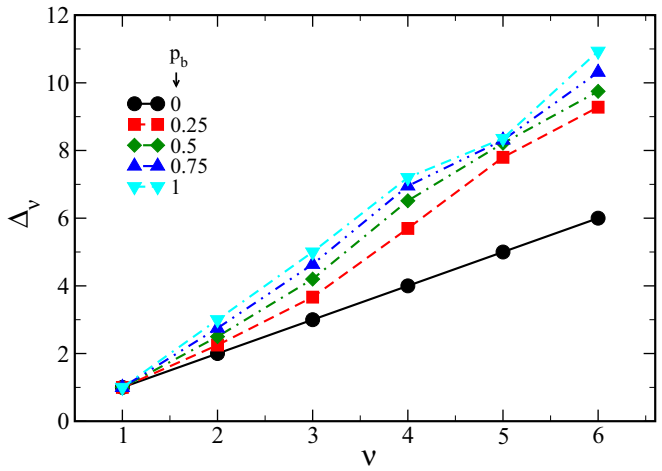

FIG. 8. The first six exact values of Δ_ν for the diluted rung model with $B = 1$ and different values of the probability p_b (given, respectively, by the numbers in the legend). In this case we have $I_A = I$, $I_B = 0$ and $B_A = B_B = B$. The lines are just guides for the eye.

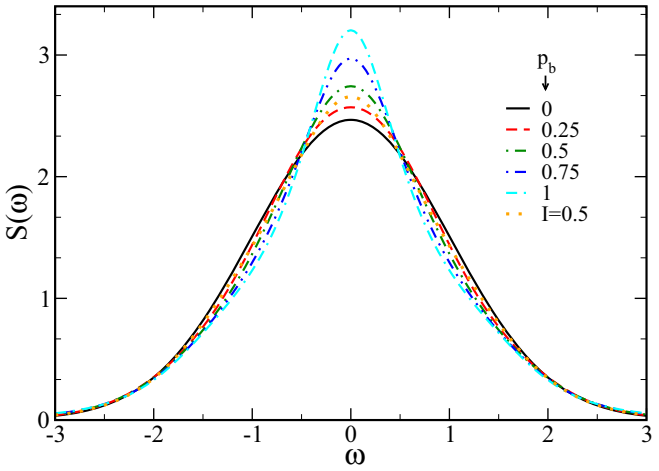

FIG. 10. Spectral functions $S(\omega)$ for the diluted rung model with $B = 1$ and different values of the probability p_b (given, respectively, by the numbers in the legend). In this case we have $I_A = I$, $I_B = 0$ and $B_A = B_B = B$. Isotropic case $I = 0.5$ is also presented for comparison purposes.

hand, when $p_b = 1$ we have the isotropic transverse Ising ladder in a homogeneous transverse field, exactly the same as $I = 1$ in the previous section. In between, the recurrants are also more or less aligned, which allows us to make an extrapolation up to 100 recurrants to obtain the corresponding temporal autocorrelation function.

In Fig. 9 the so obtained temporal autocorrelation functions $C(t)$ are displayed with $I_A = I = 1$, $I_B = 0$ and $B_A = B_B = B = 1$, for different values of the rung probability p_b. As before, the increase of p_b slower the decay of $C(t)$, because the system goes from the transverse Ising chain to the isotropic transverse Ising ladder configuration.

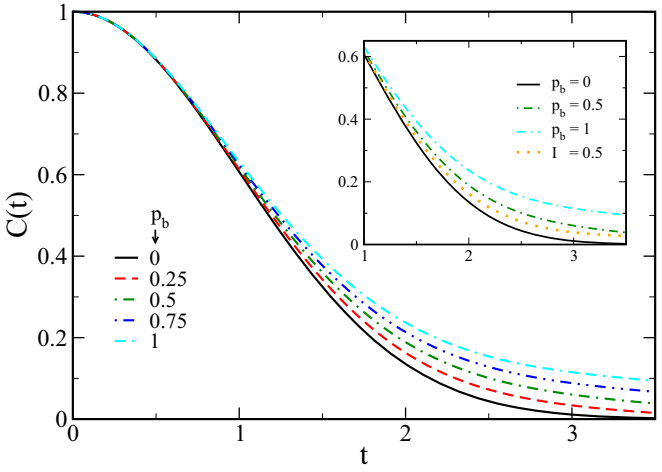

FIG. 9. Correlation functions for the diluted rung model with $I = 1$, $B = 1$, and different values of the probability p_b (given, respectively, by the numbers in the legend). The inset shows an amplified view for longer times with the inclusion of the previous section isotropic case $I = 0.5$ (dotted line) for comparison purposes. The axes labels of the main graph apply also to the inset.

The inset in Fig. 9 shows an amplified view for longer times including the isotropic case when $I = 0.5$. While $p_b = 0$ and $p_b = 1$ provide, respectively, the same results as the pure model for $I = 0$ and $I = 1$, the dynamics for $p_b = 0.5$ is different from the dynamics of the pure model with $I = 0.5$ (note that at $p_b = 0.5$, on average one has rung interaction equal to 0.5). In particular, the effect of the disorder is, in this case, to induce a slower time decay of the autocorrelation function.

The corresponding spectral functions $S(\omega)$ are displayed in Fig. 10. Increasing the number of rungs causes increasingly pronounced and narrow peaks for the spectral function curves. It can also be seen the difference on the dynamics for the random model at $p_b = 0.5$ regarding the nondisordered one.

VI. RANDOM TRANSVERSE MAGNETIC FIELD WITH $B_A \neq B_B$

Up to now, we have considered only the effects of homogeneous transverse field $B_A = B_B = B$. The central peak character has been the dominant behavior for small fields, while collective modes are present for higher values of B.

It is interesting to see, however, what should be the dynamic behavior when the transverse field is randomly distributed over the ladder. For this purpose we will consider $B_A = 0.5$, $B_B = 1.5$ and $I_A = I_B = 1$. The corresponding first three recurrants are given by

$$\Delta_1 = \overline{B_j^2},$$
$$\Delta_2 = 2J^2 + I^2,$$
$$\Delta_3 = \frac{J^2\left(\overline{B_{j+1}^2} + \overline{B_{j-1}^2} + 4J^2 + 8I^2\right) + \overline{B_j^2} I^2}{2J^2 + I^2}, \tag{25}$$

where

$$\overline{B_i^2} = p_t B_A^2 + (1 - p_t) B_B^2. \tag{26}$$

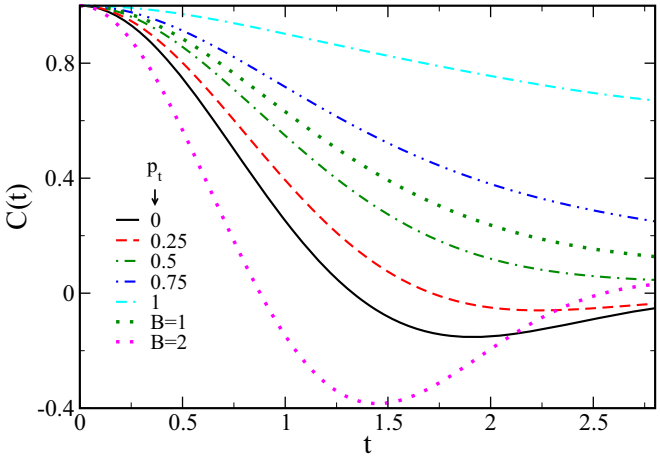

FIG. 11. Time-dependent spin autocorrelation functions $C(t)$ as a function of time t for some values of the probability p_t (given in the legend). It has been used for 100 recurrants according to the described extrapolation process. We have $B_A = 0.5$, $B_B = 1.5$, and $I = 1$. The upper green dotted line and the lower magenta dotted line are for the pure model of Sec. IV with $B_A = 1$ and $B_B = 2$, respectively.

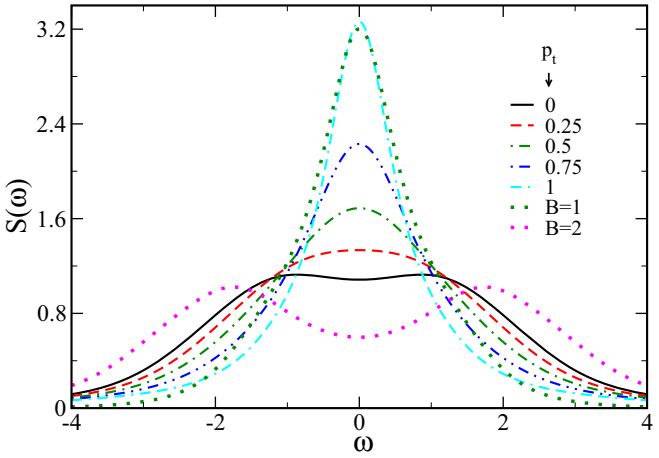

FIG. 12. Spectral functions obtained from the autocorrelation functions shown in Fig. 11.

Note that now the recurrants are a function of p_t and independent of p_b. For $p_t = 0$ and $p_t = 1$ the system corresponds to an Ising ladder in the presence of a uniform transverse field B with strength $B = 1.5$ and $B = 0.5$, respectively.

As before, the following three recurrants are also computed exactly and extrapolated to get a total of 100 to obtain the autocorrelation function. The first six recurrants are, in this case, similar to those already depicted in the previous sections.

In Fig. 11 the correlation functions $C(t)$ are displayed for several values of the probability p_t. For $p_t = 0$ and $p_t = 0.25$ the decay is faster, becomes negative, and approaches zero from below. This is because there are more sites in the presence of the higher value of the transverse field, which in turn induces a kind of precession of the spins around the field. On the other hand, for $p_t \geqslant 0.5$ the presence of the smaller field is enhanced and only a smooth decay is observed.

The autocorrelation function for $p = 0.5$ in Fig. 11 corresponds to an average transverse field $\overline{B} = 1$. The upper green dashed line in that figure corresponds to the pure case with $B = 1$, as obtained in Sec. IV. It is clearly seen that the randomness in the field affects the dynamics of the system and, contrary to the rung dilution, induces a faster decay of the correlation function.

In Fig. 11 is also shown the pure case for an even higher field $B = 2$, where the precession is still more pronounced and inducing an oscillatory behavior within the timescale of the figure.

Figure 12 shows the spectral functions $S(\omega)$ obtained from the autocorrelation functions given in Fig. 11. For $p_t \geqslant 0.25$ the central peak behavior is dominant. This is because the system is subject to less intense transverse field. For $p_t = 0$ collective modes emerge due to the stronger fields. To see this more clearly, it is also shown the spectral function for the pure case with an even stronger field $B = 2$, where the collective modes are more apparent.

The different dynamic behavior can also be seen by comparing the spectral function with $p_t = 0.5$ and the pure case for the field $B = 1$. In this case, however, the central peak behavior is unchanged. Another interesting fact is that even having 75% of stronger site fields, the central peak behavior is the dominant one. It means that, in this case, even a small concentration of weaker fields is sufficient to destroy the collective modes. For different values of the distribution parameters, different concentrations will separate the central peak to the collective mode regimes.

As a final comment in this case, it has been noticed that, contrary to what happens in the diluted transverse field Ising chain at zero temperature, where small randomness improves the order [62], the ladder at infinite temperature always has a faster decay as the concentration of the larger field increases.

VII. RANDOMLY CORRELATED RUNG INTERACTION AND TRANSVERSE FIELD

In all the above examples, either the rung interaction or the transverse field has been considered randomly distributed over the ladder. Naturally, both distributions can also be studied at the same time. The main features of the dynamics will be where the interaction or the field will prevail. This instance will be treated in the next section. However, one interesting situation is when there is a correlation between both probability distributions. Assume, for example, that

$$P_b(I_i) = p\delta(I_i) + (1-p)\delta(I_i - I), \tag{27}$$

$$P_t(B_i) = p\delta(B_i - B) + (1-p)\delta(B_i), \tag{28}$$

where the probability p is the same for both distributions. It means that when $p = 0$, as was discussed in the beginning of Sec. VI, one has a classical spin ladder that has no dynamics for any value of the rung interaction and the autocorrelation function is always $C(t) = 1$. On the other hand, when $p = 1$, one has the one-dimensional transverse Ising model, since there is no rung interaction. Thus, intermediate values of p lead to a competition between the classical and quantum behavior on the dynamics of the system.

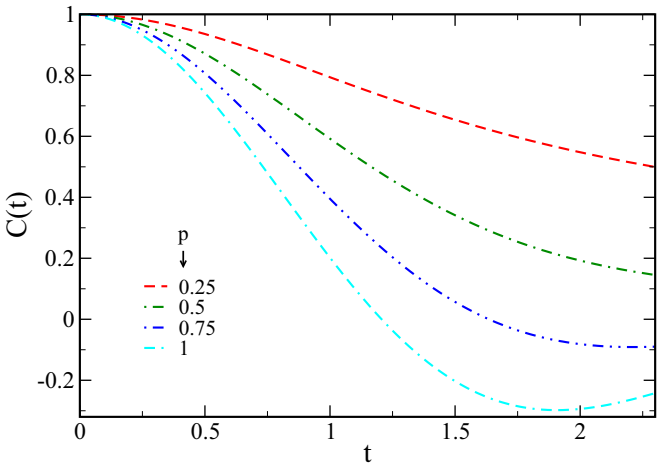

FIG. 13. Time-dependent spin autocorrelation functions $C(t)$ as a function of time t for some values of the probability p (shown in the legend). Here 100 recurrants have been used according to the described extrapolation process. We have $I = 1.5$ and $B = 1.5$ from Eqs. (27) and (28), respectively.

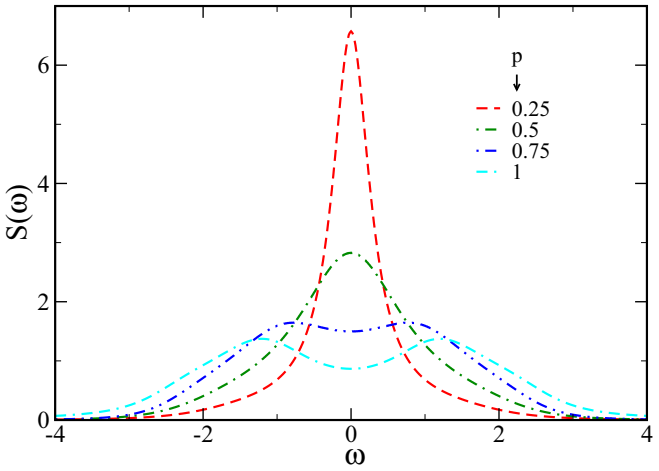

FIG. 14. Spectral functions obtained from the autocorrelation functions shown in Fig. 13.

The first three recurrants with the probability distributions (27) and (28) are given by

$$\Delta_1 = pB^2,$$
$$\Delta_2 = 2J^2 + (1-p)I^2,$$
$$\Delta_3 = \frac{J^2[2pB^2 + 4J^2 + 8(1-p)I^2] + p(1-p)B^2I^2}{2J^2 + (1-p)I^2}. \tag{29}$$

Again, the remaining three Δ_ν are also exactly computed, and the extrapolation process provides the rest of 100 recurrants.

We have considered here a higher transverse field $B = 1.5$ and a higher rung interaction $I = 1.5$. As was discussed in the previous section, this value of the field is able to introduce collective modes of the spins around B.

The time-dependent autocorrelation functions $C(t)$ are displayed in Fig. 13 for some values of the probability p. The case $p = 0$ is not shown because the system has no dynamics. As p increases, the decay becomes faster, and for $p \geqslant 0.75$, $C(t)$ approaches zero from negative values. The tendency of the quantum fluctuations, for these values of the rung interaction and transverse field, is clearly to induce a faster decay of the autocorrelation function.

The corresponding spectral function $S(\omega)$, obtained from the autocorrelation functions in Fig. 13, is shown in Fig. 14. It is clearly seen that the central peak mode, for small values of the probability p, changes to collective modes for $p \geqslant 0.75$. This change in the dynamic behavior is associated with the fact that, at the same time that quantum fluctuations are introduced in the system, more sites feel the presence of the transverse field, which, in turn, induces precession of the spins about B.

VIII. RANDOM RUNG INTERACTION AND RANDOM TRANSVERSE FIELD: $I_A = 0.5$, $I_B = 1.5$ AND $B_A = 0.5$, $B = 1.5$

Finally, as a last example we consider, simultaneously and independently, disorder in the rung bonds and in the transverse external fields given by Eqs. (2) and (3), respectively. As in this instance we have too many parameters to be taken into account, we will restrict ourselves to the case where $I_A = 0.5$, $I_B = 1.5$ and $B_A = 0.5$, $B = 1.5$, with $p_b = p_t$. From these results it would be possible to have a general picture of the dynamical behavior for different values of parameters and, at the same time, to make a comparison with the results obtained in previous sections.

Figure 15 depicts some results for the autocorrelation function as a function of time and different concentrations given by the thinner lines shown in the legend. $p_b = p_t = 0$ is equivalent to a pure transverse Ising ladder with rung interaction $I_B = 1.5$ and transverse field $B_B = 1.5$. The decay is faster in this case and becomes slower as the concentration increases in the direction to the pure system with $p_b = p_t = 1$, equivalent to a ladder with $I_B = 0.5$ and $B_B = 0.5$. One can notice, from the previous sections, that for a given value of a transverse field, the decay is slower as the rung interactions increases, while for a given value of the rung interaction the decay is faster as the transverse field increases. However, looking at the behavior of the autocorrelation function for $I_B = 0.5$ and $B_B = 0.5$, and comparing to the behavior for $I_B = 1.5$ and $B_B = 1.5$, we can see that by increasing the values of rung interaction and transverse field by the same amount, the transverse field effects prevail over the rung interaction ones since the decay becomes slower.

An illustrative case is when $p_b = p_t = 0.5$, meaning that, on average, one has $\bar{I} = 1$ and $\bar{B} = 1$. This situation can also be compared to autocorrelation functions obtained in previous sections, which are depicted in Fig. 15 by the thicker lines (a), (b), and (c). The brown dotted line (a) corresponds to the pure model from Sec. IV with $I_A = I_B = 1$ and $B_A = B_B = 1$. Starting from this pure case, if disorder is introduced only into the rung bonds with $I_A = 0.5$, $I_B = 1.5$, and $p_b = 0.5$, leaving

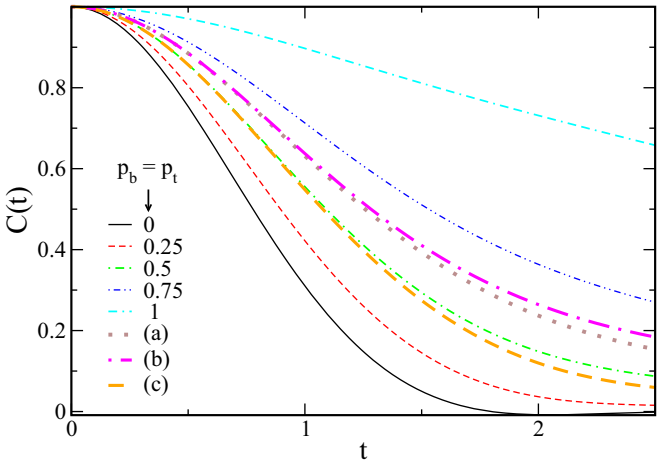

FIG. 15. Spin autocorrelation functions $C(t)$ as a function of time t for some values of the probability $p_b = p_t$ (shown in the legend and represented by the thinner lines, where we have $I_A = 0.5$ and $I_B = 1.5$ for the rung interactions and $B_A = 0.5$ and $B_B = 1.5$ for the transverse field distributions). The thicker lines represent the following: (a) brown dotted line, uniform transverse Ising ladder of Sec. IV with $I_A = I_B = 1$ and $B_A = B_B = 1$; (b) magenta long-dashed-dotted line, uniform transverse field with rung disorder of Sec. V with $B_A = B_B = B = 1$, $I_A = 0.5$, $I_B = 1.5$, and $p_b = 0.5$; (c) orange long-dashed line, uniform rung interaction and random transverse field of Sec. VI with $I_A = I_B = 1$, $B_A = 0.5$, $B_B = 1$, and $p_t = 0.5$.

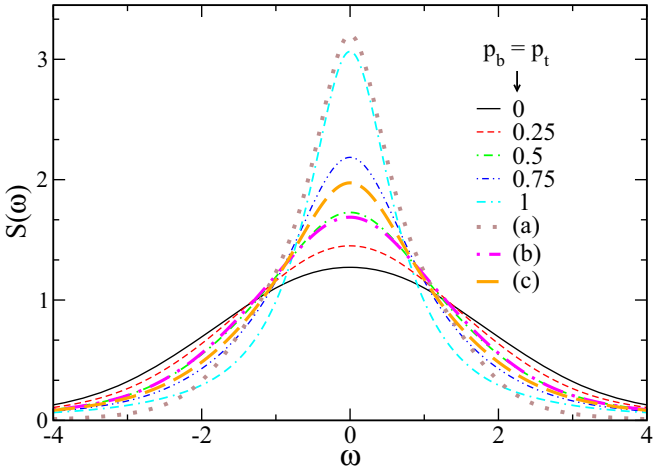

FIG. 16. Spectral functions obtained from the autocorrelation functions shown in Fig. 15, definitions of the lines (a), (b), and (c) are given in the caption of Fig. 15.

the field homogeneous, $B_A = B_B = B = 1$, we see from the magenta long-dashed-dotted line (b) that the decay of the autocorrelation function becomes slower, as already discussed in Sec. V. On the other hand, if disorder is introduced only into the fields with $B_A = 0.5$, $B_B = 1.5$, and $p_t = 0.5$, leaving the rung homogeneous $I_A = I_B = B = 1$, we see from the orange long-dashed line (c) that the decay of the autocorrelation function becomes faster, as already discussed in Sec. VI. However, if the disorder is introduced simultaneously in both rung interaction and transverse field, one can see that the faster decay effect from the field still prevails, as can be seen by the green thinner dashed-dotted line for $p_b = p_t = 0.5$.

The curves for spectral densities, presented in Fig. 16, also exhibit different behaviors depending on interactions and fields. However, in all cases considered here there is the presence of a single central peak. Collective modes will appear for larger values of B_B.

IX. CONCLUDING REMARKS

In this work the dynamics of the Ising ladder with random rung interactions and random transverse magnetic fields has been studied using the recurrance relations method. Bimodal distributions for both rung and transverse field have been considered. The time-dependent z-component spin autocorrelation function and the corresponding spectral function have been computed. Different choices for the Hamiltonian parameters and probability distributions, which correspond to different types of models, have been analyzed in more detail.

It has been noticed that, in general, there is a competition between the rung interaction and the transverse field. While the increase of the former develops a clear central peak and drives the system to a more classical behavior, the latter leads to collective modes for strong enough transverse fields and enhances the quantum fluctuations. The competition between both interactions comes not only from different intensities in the pure case, but also from the probability distributions in the random and correlated case.

In order to have an additional view of the competition between rung interaction and transverse field, the spectral functions for further two particular cases are shown in Fig. 17. The full line in that figure corresponds to the ladder with rung interactions $I_A = I_B = I = 1.5$ in the presence of a diluted transverse field with 25% of the sites having no field ($B_A = 0$)

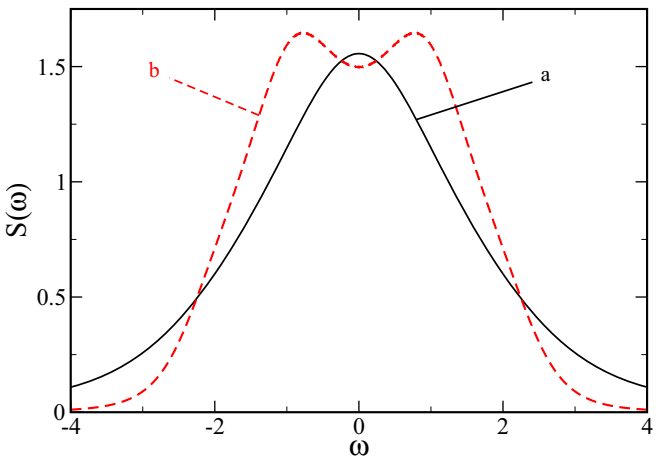

FIG. 17. Spectral function for two particular cases. The full line (a) corresponds to the ladder with rung interactions $I_A = I_B = I = 1.5$ in the presence of a diluted transverse field with 25% of the sites having no field ($B_A = 0$) and 75% of the sites having a field of strength $B_B = B = 1.5$. The dashed line (b) corresponds to the correlated random case, with the same transverse field concentrations as in (a), but now having only 25% of rung interactions $I = 1.5$ and 75% disconnected rungs $I = 0$ [it is the $p = 0.75$ case of Eqs. (27) and (28)].

and 75% of the sites having a field of strength $B_B = B = 1.5$. One can clearly see that, although the field is 25% diluted, the rung interaction $I = 1.5$ is sufficient to keep the central peak behavior of $S(\omega)$. However, upon an additional dilution of 75% of the rung interactions [equivalent to having, in Eqs. (27) and (28), probability $p = 0.75$], the collective modes are induced, as is shown by the dashed line in Fig. 17.

As a final remark, it has been noticed that the dynamical behavior of the random model is different from the pure model at the mean value of the corresponding random variable. For instance, with a homogeneous transverse field, the decay of the pure model at the mean rung interaction is faster than the random rung interaction model. On the other hand, for homogeneous rung interaction, the decay of the pure model at the mean transverse field is slower than the random transverse field model. When both randomness are simultaneously present, the disorder effect induced by the transverse field prevails and the autocorrelation function has a faster decay.

ACKNOWLEDGMENTS

Special thanks are addressed to Wescley Luiz de Souza, Paulo Henrique Lana Martins, and Érica de Mello Silva for kindly providing the program to obtain the spectral functions. Financial support from CNPq, CAPES, and FAPEMIG is also acknowledged.

[1] D. Hirobe, M. Sato, T. Kawamata, Y. Shiomi, K. Uchida, R. Iguchi, Y. Koike, S. Maekawa, and E. Saitoh, Nature Phys. **13**, 30 (2017).
[2] D. C. Johnston, J. W. Johnson, D. P. Goshorn, and A. J. Jacobson, Phys. Rev. B **35**, 219 (1987).
[3] M. Hagiwara, H. A. Katori, U. Schollwock, and H. J. Mikeska, Phys. Rev. B **62**, 1051 (2000).
[4] H. Arisawa, H. Shim, S. Daimon, S. Takahashi, T. Ono, and E. Saitoh, Nat. Commun. **13**, 2440 (2022).
[5] Z. Y. Zhao, X. G. Liu, Z. Z. He, X. M. Wang, C. Fan, W. P. Ke, Q. J. Li, L. M. Chen, X. Zhao, and X. F. Sun, Phys. Rev. B **85**, 134412 (2012).
[6] B. Grenier, S. Petit, V. Simonet, E. Canévet, L.-P. Regnault, S. Raymond, B. Canals, C. Berthier, and P. Lejay, Phys. Rev. Lett. **115**, 119902(E) (2015).
[7] M. Kenzelmann, R. Coldea, D. A. Tennant, D. Visser, M. Hofmann, P. Smeibidl, and Z. Tylczynski, Phys. Rev. B **65**, 144432 (2002).
[8] Y. Cui, H. Zou, N. Xi, Z. He, Y. X. Yang, L. Shu, G. H. Zhang, Z. Hu, T. Chen, R. Yu, J. Wu, and W. Yu, Phys. Rev. Lett. **123**, 067203 (2019).
[9] Y. Pogoryelov, J. Magnetics **9**, 97 (2004).
[10] E. Gomonay and Y. Pogoryelov, IEEE Trans. Magnetics **41**, 2598 (2005).
[11] J. A. Plascak and S. R. Salinas, Physica Status Solidi (b) **113**, 367 (1982).
[12] J. A. Plascak, A. S. T. Pires, and F. C. Sá Barreto, Solid State Commun. **44**, 787 (1982).
[13] J. A. Plascak, F. C. Sá Barreto, and A. S. T. Pires, Phys. Rev. B **27**, 523 (1983).
[14] J. A. Plascak, F. C. Sá Barreto, A. S. T. Pires, and L. L. Gonçalves, J. Phys. C **16**, 49 (1983).
[15] O. Derzhko and T. Krokhmalskii, Ferroelectrics **192**, 21 (1997).
[16] O. Derzhko, T. Krokhmalskii, and J. Stolze, J. Phys. A: Math. Gen. **33**, 3063 (2000).
[17] P. G. de Gennes, Solid State Commun. **1**, 132 (1963).
[18] T. Niemeijer, Physica **36**, 377 (1967).
[19] U. Brandt and K. Jacoby, Z. Phys. B **25**, 181 (1976).
[20] U. Brandt and K. Jacoby, Z. Phys. B **26**, 245 (1977).
[21] H. W. Capel and J. H. H. Perk, Physica A **87**, 211 (1977).
[22] M. Karbach and G. Müller, Phys. Rev. B **62**, 14871 (2000).
[23] M. Karbach, D. Biegel, and G. Müller, Phys. Rev. B **66**, 054405 (2002).
[24] J. Sato, M. Shiroishi, and M. Takahashi, J. Phys. Soc. Jpn. **73**, 3008 (2004).
[25] R. Hagemans, J.-S. Caux, and J. M. Maillet, in *Proceedings of the "Tenth Training Course in The Physics of Correlated Electron and High-Tc Superconductors,"* Salerno, Italy, October 2005, AIP Conf. Proc. No. 846 (AIP, New York, 2006), pp. 245–254.
[26] V. Ohanyan and A. Honecker, Phys. Rev. B **86**, 054412 (2012).
[27] J. Strečka, O. Rojas, T. Verkholyak, and M. L. Lyra, Phys. Rev. E **89**, 022143 (2014).
[28] L. Gálisová, J. Phys.: Condens. Matter **28**, 476005 (2016).
[29] J. Torrico, M. Rojas, S. M. de Souza, and O. Rojas, Phys. Lett. A **380**, 3655 (2016).
[30] R. C. Alécio, J. Streíka, and M. L. Lyra, J. Magn. Magn. Mater. **451**, 218 (2018).
[31] L. Gálisová and D. Knežo, Phys. Lett. A **382**, 2839 (2018).
[32] H. ArianZad, V. Ohanyan, A. Zoshki, and J. Streíka, Phys. Rev. E **108**, 044132 (2023).
[33] O. Derzhko and T. Krokhmalskii, Phys. Rev. B **56**, 11659 (1997).
[34] O. Derzhko and T. Krokhmalskii, Physica Status Solidi (b) **208**, 221 (1998).
[35] O. Derzhko, *Condensed Matter Physics in the Prime of the 21st Century* (World Scientific, Singapore, 2008), pp. 35–87.
[36] O. Derzhko, T. Krokhmalskii, and T. Verkholyak, J. Magn. Magn. Mater. **157–158**, 421 (1996).
[37] T. Verkholyak, O. Derzhko, T. Krokhmalskii, and J. Stolze, Phys. Rev. B **76**, 144418 (2007).
[38] O. Derzhko, T. Krokhmalskii, and J. Stolze, J. Phys. A **35**, 3573 (2002).
[39] J. Florencio and O. F. de Alcantara Bonfim, Front. Phys. **8**, 557277 (2020).
[40] M. E. S. Nunes, E. M. Silva, P. H. L. Martins, J. Florencio, and J. A. Plascak, Physica A **541**, 123683 (2020).
[41] E. M. Silva, Phys. Rev. E **92**, 042146 (2015).
[42] M. E. S. Nunes, J. A. Plascak, and J. Florencio, Physica A **332**, 1 (2004).
[43] I. Sawada, Phys. B: Condens. Matter **329–333**, 998 (2003).
[44] J. Florencio, M. H. Lee, and J. B. Hong, Braz. J. Phys. **30**, 725 (2000).
[45] C. B. Krimphoff, M. Haque, and A. M. Lauchli, Phys. Rev. B **95**, 144308 (2017).

[46] X.-J. Yuan, C.-Y. Wang, X.-M. Kong, J.-F. Zhao, H. Wang, H.-X. Bu, J. Magn. Magn. Mater. **572**, 170632 (2023).
[47] M. H. Lee, Phys. Rev. Lett. **49**, 1072 (1982).
[48] M. H. Lee, Phys. Rev. B **26**, 2547 (1982).
[49] S. J. Leon, Å. Björck, and W. Gander, Num. Linear Algebra Appl. **20**, 492 (2013).
[50] J. Matthews and R. L. Walker, *Mathematical Methods of Physics* (Benjamin, Reading, MA, 1970).
[51] R. Kubo, J. Phys. Soc. Jpn. **12**, 570 (1957).
[52] R. Kubo, Rep. Prog. Phys. **29**, 255 (1966).
[53] W. L. de Souza, E. de Mello Silva, and P. H. L. Martins, Phys. Rev. E **101**, 042104 (2020).
[54] V. S. Viswanath and G. Müller, J. Appl. Phys. **67**, 5486 (1990).
[55] P. R. C. Guimarães, J. A. Plascak, O. F. de Alcantara Bonfim and J. Florencio, Phys. Rev. E **92**, 042115 (2015).
[56] X.-J. Yuan, X.-M. Kong, Z.-B. Xu, and Z.-Q. Liu, Physica A **389**, 242 (2010).
[57] J. Florencio Jr., S. Sen, and Z.-X. Cai, J. Low. Temp. Phys. **89**, 561 (1992).
[58] J. Florencio and F. C. Sá Barreto, Phys. Rev. B **60**, 9555 (1999).
[59] J. Florencio Jr., O. F. A. Bonfim, and F. S. Barreto, Physica A **235**, 523 (1997).
[60] J. C. Xavier, R. G. Pereira, M. E. S. Nunes, and J. A. Plascak, Phys. Rev. B **105**, 024430 (2022).
[61] M. E. S. Nunes, F. W. S. Lima, and J. A. Plascak, Entropy **25**, 1665 (2023).
[62] O. Derzhko, T. Krokhmalskii, and T. Verkholyak, Philos. Mag. B **76**, 855 (1997).